16TH EUROPEAN CONFERENCE ON EARTHQUAKE ENGINEERING
THESSALONIKI 18 - 21 JUNE 2018

EVALUATION OF EARTHQUAKE-INDUCED LANDSLIDE HAZARD IN THE ISLAND OF LEFKADA, IONIAN SEA, GREECE

George PAPATHANASSIOU[1], Sotiris VALKANIOTIS[2], Athanassios GANAS[3]

ABSTRACT

The island of Lefkada, Greece has been repeatedly struck by moderate earthquakes (moment magnitude range 6.2-6.6). According to the post-earthquake reconnaissance reports prepared after the earthquakes, the triggered environmental effects are widespread causing structural damages on the road network, port facilities and buildings. The dominant type of earthquake-induced ground failures are usually slope failures including rockfalls, rockslides and landslides while medium-size liquefaction phenomena are also reported. The goal of this article is to evaluate the earthquake-induced landslide hazard and to provide a relevant hazard map that could be used by urban planners and designers in order to avoid the hazardous zones. This was achieved by computing the joint probability, by multiplying the temporal probability by the probability of landslide occurrence conditioned on magnitude exceedance. In addition, the compiled earthquake-induced landslide map was compared with the locations of slope failures triggered by a recent earthquake that occurred on November 17, 2015. The outcome by this comparison is that the delineated slope failures areas in this study are in agreement with the spatial distribution of the 2015 co-seismic landslide occurrences.

Keywords: earthquake; landslide; hazard; probability; Lefkada

1. INTRODUCTION

Landslide hazard was defined by Varnes (1984) as the probability of occurrence within a specified period of time and within a given area of a potentially damaging phenomenon. Thus, having estimated the information regarding "when" e.g. temporal probability of earthquake triggering landslide events and the relevant information of "where" e.g. spatial probability of landslides, the earthquake-induced landslide hazard can be evaluated by estimating the joint probability of the previous mentioned ones (Jaiswal et al., 2010). Guzzetti et al. (2005) stated that landslide magnitude or density should also be included as an additional parameter in the equation used for the estimation of landslide hazard.

Taking into account that a landslide can be triggered by rainfall, earthquakes, volcanic eruption and man-made activities, it is mandatory to initially define the examined triggered factor. In particular, threshold values, defined as the minimum magnitude that should be exceeded for the initiation of landslides must be evaluated in conjunction with the spatial probability of the slope failures.

This study deals with the estimation of landslide hazard in the island of Lefkada (Ionian Sea, Greece) and particularly with the earthquake-induced ones. It was decided to focus on this specific factor because the island of Lefkada is often struck by moderate earthquakes of M>6.0 (e.g. Louvari et al., 1999; Papathanassiou et al., 2005) that triggered widespread slope failures including rock falls, rock slides and landslides as the one of magnitude M6.5 that occurred on November 17, 2015 onshore the island of Lefkada (Ganas et al., 2016).

[1]Assistant Professor, Dept Civil Engineering, Democritus University of Thrace, Xanthi, Greece, gpapatha@auth.gr
[2] Dr., Koronidos 9, Trikala, Greece, valkaniotis@yahoo.com
[3]Research Director, Institute of Geodynamics, National Observatory of Athens, Greece, aganas@noa.gr

In particular, having estimated the temporal probability (Papathanassiou et al., 2011) and the landslide susceptibility (Papathanassiou et al., 2013), the goals of this study are the estimation of the i) probability of landslide occurrence conditioned on magnitude exceedance and the ii) development of a quantitative model of landslide hazard assessment for two different earthquake scenario magnitudes M5.3 and M6.0 for a return period from 10 to 500 years.

2. THE ISLAND OF LEFKADA

The geology of the Lefkada island, comprises: (1) a carbonate sequence of the Ionian zone, (2) limestone of Paxos (Apulia) zone restricted in the SW peninsula of the island, (3) few outcrops of ionian flysch (turbidites) and Miocene marls-sandstones mainly in the northern part of the island (Cushing, 1985; Rondoyanni-Tsiambaou, 1997). The boundary between the two different geological zones – Ionian and Paxos, runs in an approximate NW- SE direction through this region and outcrops onshore south-central Lefkada Island near Hortata village, in the form of a buried thrust fault by scree and late Quaternary deposits (Papathanassiou et al., 2017). Pleistocene and especially Holocene coastal deposits are extended in the northern edge of Lefkada, where the homonym capital town is founded, in the valley of Vassiliki and in the coast Nydri.

Regarding the seismicity, it is pointed out that the island of Lefkada is considered as one of the most tectonically active areas in Europe being part of the high seismicity Ionian Sea area, and particularly due to the complex crustal deformation resulting from the subduction of the African plate towards NE and the Apulian platform continental collision further to the northwest (Hatzfeld et al., 1995; Clement et al., 2000; Ganas et al., 2013). The main active tectonic structure, is the 140 km long dextral strike-slip Cephalonia-Lefkada Transform fault (Fig. 1) (CTF; Scordilis et al., 1985; Louvari et al., 1999; Sachpazi et al., 2000), which has a GPS slip-rate bracketed between 10 and 25 mm/yr (Pérouse et al., 2012). The steep morphology on the western part of the island, where most of slope failure cases are reported is due to this offshore CTF and its onshore sub-parallel fault; the Athani-Dragano fault (Cushing, 1985; Rondoyanni et al., 2007). The latter one is a NNE-SSW striking fault forming a narrow elongated continental basin, very well expressed in the region's morphology and marked on satellite images and aerial photos.

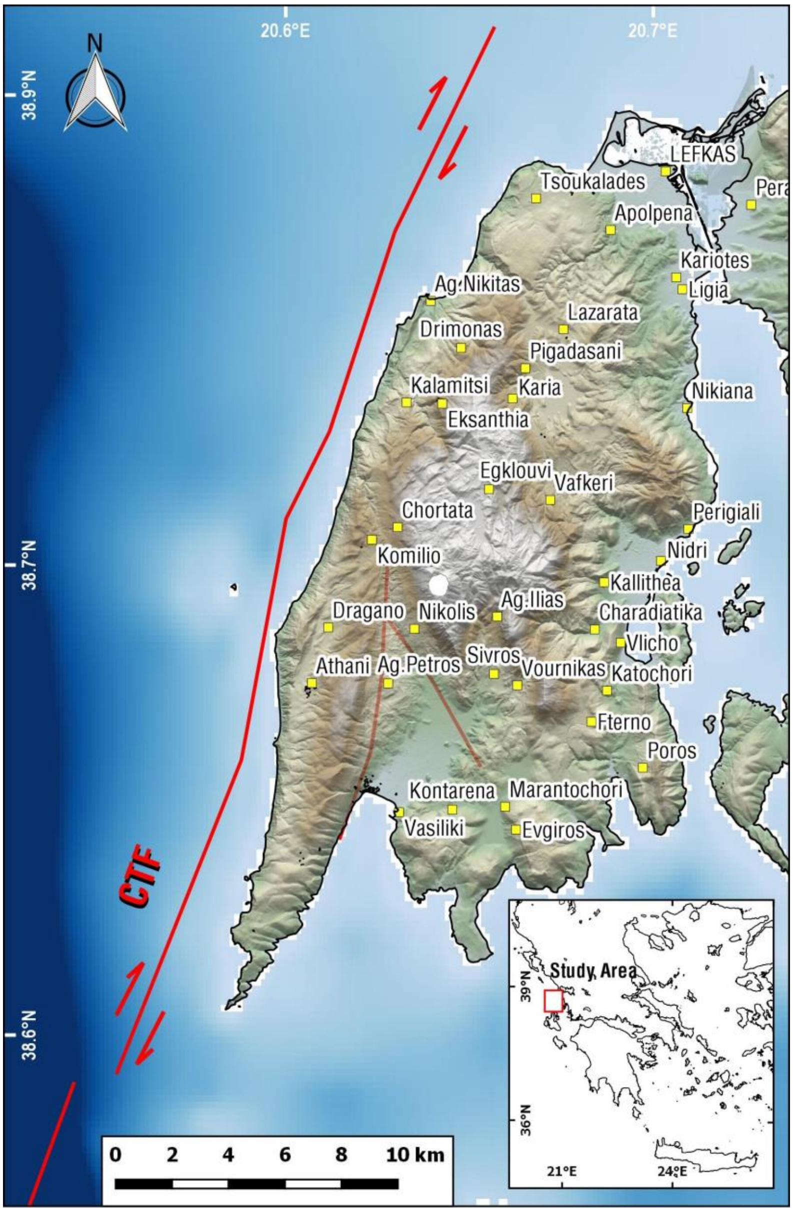

Figure 1. Map of the island of Lefkada showing the Cephalonia-Lefkada Transform Fault CTF

3. EVALUATION OF TEMPORAL PROBABILITY

In order to evaluate the temporal probability of earthquake-induced landslides in the island of Lefkada, Papathanassiou et al. (2011) decided to follow the procedure proposed by (Jaiswal and van Westen, 2009); the temporal probability was estimated as a joint probability by multiplying the exceedance probability of earthquake threshold per decade by the probability of landslide occurrence once the threshold has been exceeded.

In particular, having estimated the probability of occurrence of the triggering threshold, the probability of landslide occurrence can be assumed since in this simplified model landslides always occur when magnitude M exceeds magnitude threshold Mt and never occur when the value of M is lower or equal to Mt (Jaiswal and van Westen, 2009). However, the threshold may be exceeded without triggering a landslide. In order to overcome this, Floris and Bozzano (2008) suggested to take into account the conditional probability of a given threshold exceedance [P{M>Mt}] and the probability of occurrence of a landslide [P{L}], given the exceedance. Thus, the probability of occurrence of both {M>Mt} and {L} is equal to the probability of {M>Mt} multiplied by the probability of occurrence of {L}, assuming that the {M>Mt} has already occurred (Jaiswal and van Westen, 2009). The probability of {M>Mt} can be obtained by determining the exceedance probability of the earthquake magnitude threshold using a Poisson (recurrence) model and the probability of {L M>Mt} relies on the frequency of occurrence of landslides after the threshold has been exceeded (Jaiswal et al, 2010).

Regarding the case of the island of Lefkada, the temporal probability of earthquake-induced landslide was estimated using information provided by historical reports describing environmental effects triggered by earthquakes. The threshold values that have been employed in this model are M=5.3, suggested by Papadopoulos and Plessa (2000), and M=6.0, since the seismic catalogues in Greece can be characterized as complete and reliable regarding the description and report of secondary effects for earthquake magnitude M>6. Furthermore, in order to ensure a reliable and accurate evaluation of the earthquake magnitude, only the events that occurred during the instrumental period of seismicity from 1911 to 2010 were taken into account.

The outcome provided by Papathanassiou et al. (2011) is that the mean recurrence interval per decade between successive threshold exceedance is 0.48 and 1.66 for earthquake magnitudes M=5.3 and M=6.0, respectively. Taking into account that the probability of occurrence of landslide after the threshold has been exceeded is 0.23 and 0.83 for M>5.3 and M>6.0, the estimated temporal probability of earthquake-induced landslides for different time periods, from 10 to 500 years, ranges from 0.2 to 0.23 for earthquake magnitudes M>5.3 and from 0.37 to 0.83 for magnitude M>6.0 (Table 1).

Table 1. Corresponding values of annual exceedance probability (AEP) and temporal probability of earthquake-induced landslides computed for a time equal to 10, 25, 50, 75, 100 and 500 years (Papathanassiou et al., 2011).

aep	**aep**	**years**	**temporal probability**	
(M>5.3)	**(M>6.0)**		**M>5.3**	**M>6.0**
0.877	0.451	10	0.208	0.375
0.994	0.776	25	0.236	0.647
0.999	0.950	50	0.238	0.791
0.999	0.988	75	0.238	0.824
0.999	0.997	100	0.238	0.831
1	1	500	0.238	0.833

4. COMPILATION OF THE INVENTORY MAP

Detailed, comprehensive inventories of landslides triggered by earthquakes are the essential parts of seismic landslide hazard analyses. In particular, the compilation of the inventory map and the evaluation of the density of landslides should be based on a seismic event and particularly an event that fulfill two basic criteria; occurred on instrumental period and existence of a reliable and accurate post-earthquake field survey. Therefore, for the framework of this study, it was decided to “use” the 2003 earthquake (Mw=6.3, depth h=12km; Papadopoulos et al., 2003) that occurred few kilometers offshore the island of Lefkada and to compile a relevant inventory map based on a post-earthquake reconnaissance survey conducted a few days after the event (Papathanassiou et al. 2005) and cloud-free satellite imagery from Google Earth acquired on 19th December of 2005. Afterwards, a vector-to-raster conversion was undertaken to provide raster data of landslide areas with 10 m by 10 m pixels.
Furthermore, a second pre-earthquake inventory map was developed using images acquired on June of 2003, two months before the earthquake. This map was developed in order to validate the landslide susceptibility map, as it is briefly described in the next session. All the images that were used in the study of Papathanassiou et al. (2013) meet the criteria proposed by Harp et al. (2011) since i) they covered the entire area of the island, ii) are continuous and cloud-free, and iii) allow the on-screen digitization of the margins of landslides.

Papathanassiou et al. (2013) highlighted that in the island of Lefkada, the dominant reported types of landslides is rock falls and slides and is frequently observed in steep slopes of sedimentary rocks. The distribution of landslides is dense in the western part of the island, mainly in coastal zone. This is resulted due to the high level of weathering of the sedimentary rocks at the west and northwest-facing slopes due to the precipitation and the dominant direction of wind in the island of Lefkada, and the recent tectonic activity in the area that highly jointed the limestones decreasing their mechanical properties (Papathanassiou et al. 2013).

The surface of the study area (island of Lefkada) is 301.06 km^2 while the percentage of the area affected by landslides is 1.05% (3.17 km^2) and 0.59% (1.8 km^2) based on data acquired after (2005) and before (2003) the triggering event, respectively.

5. ASSESMENT OF LANDSLIDE SUSCEPTIBILITY

Having compiled the landslide inventory map after the 2003 event, the prone to landslides areas were delineated and the relevant susceptibility in the island of Lefkada was assessed. The spatial distribution of landslides was statistically analyzed in relation to the geology and topography for investigating their influence to landsliding. This was accomplished by overlaying these causal factors as thematic layers with landslide distribution data. Afterwards, weight values of each factor were calculated using the landslide index method and relevant maps were compiled.

The maps were normalized and classified into equal areas and grouped into 10 classes e.g. delineating relevant susceptibility areas. The highest susceptibility area covers the 1.65% of the total study area and the landslide activity is 38.36% of the total one. The lowest susceptibility area covers the 7.71% of the study area and concentrates the 0.01% of the total landslide area.

The validation of this map was accomplished using a second inventory map compiled based on satellite imagery acquired before the 2003 event. The spatial distribution of the second inventory map was overlaid to the susceptibility map and statistically analyzed. The resulted prediction rate curve indicates that within 10% of the susceptibility map, more than 85% of the landslides could be predicted. In addition, 30% of the susceptibility map predicts more than 90% of landslides.

For facilitating the reader, the susceptibility classes 1 to 7 have been regrouped in a single class while the classes 8, 9 and 10 (high susceptibility) are colored as orange, red and deep red (Fig. 2). In the same figure is also plotted the spatial distribution of the location of the slope failures (blue circles) triggered by the November 17, 2015 earthquake M6.5. The event triggered environmental effects that were mainly mapped at the western part of the island while moving towards the eastern part, the severity of the earthquake-induced failures decreased. The most characteristic geological effects that were triggered by the 2015 earthquake were slope failures including rock falls, rock slides and landslides with a spatial density following an exponential increase with slope-angle and decreases for values larger than 55° (Papathanassiou et al., 2017).

Comparing the spatial distribution of the location of earthquake-induced slope failures (Fig. 2), it is clearly shown, that the sites where these types of geological failures were triggered are in agreement with the areas that have been delineated as high susceptible to slope failures. In addition, focusing on the areas of higher density of these phenomena e.g. western coastal area of the island of Lefkada, it can be seen that are strongly related to the delineated zones 9 and 10 of susceptibility.

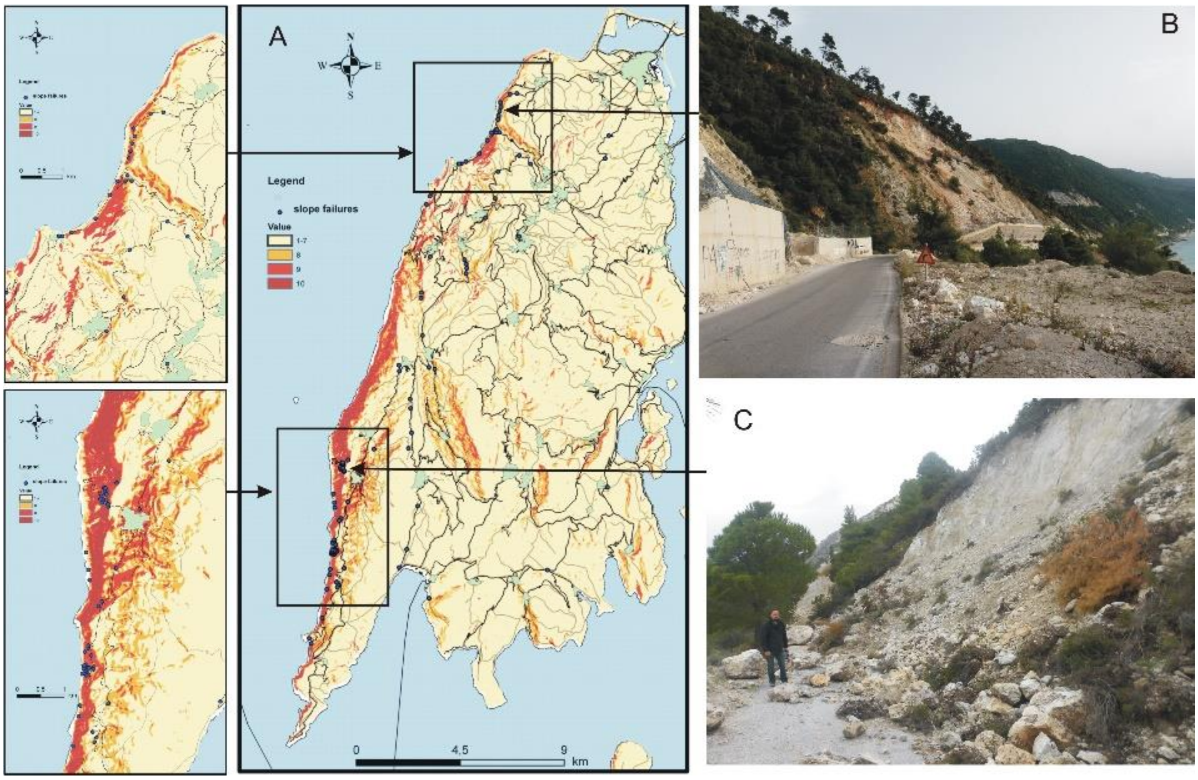

Figure 2. Landslides susceptibility map developed by Papathanassiou et al. (2013) and spatial distribution of earthquake-induced slope failures triggered by the 2015 event (blue dots). On the left it is shown the correlation of the slope failures with the published susceptibility map at the areas that were strongly affected by the 2015 earthquake. On the right are shown two photos taken on November 2015 (photo c) and on April 2016 (photo b) within the most heavily damaged areas

6. EVALUATING THE CONDITIONAL PROBABILITY

However, as it has been previously mentioned, the compilation of the landslide susceptibility map is considered as a qualitative evaluation since in order to evaluate the hazard within an area the joint probability of temporal and the conditional probability must be taken into account. The computation of the former parameter, temporal probability, was previously described while in this section is going to be presented the procedure that was followed in order to estimate the latter parameter e.g. probability of landslide occurrence conditioned on magnitude exceedance for each susceptibility class.

In order to achieve this, it was decided to apply the two-stage strategy method proposed by Chung and Fabri (2003). The first stage, assessing the ten susceptibility classes, was presented by Papathanassiou et al. (2013) and the second one, which is one of the goals of this study, concerns the evaluation of conditional probability. In particular, a scenario was developed assuming that a house of size 10m × 10m (100m^2), that can be considered as a typical Greek residential house, was built within the most hazardous zone. Afterwards, following the recommendations of Chung and Fabri (2003), the conditional probability per class, prob_i, that a future landslide will affect the house has to be estimated within the desired period of time. The value of prob_i is estimated based on the following regression:

$$\text{prob}_{\,i} = 1 - (1 - p_\gamma)^{\frac{n\alpha}{n\gamma}\kappa} \qquad (1)$$

Where nα is the number of pixels in the affected area expected as future landslides, nγ is the number of pixels in the hazard class, p_γ is the corresponding probability of the hazard class in the prediction-rate curve and κ is the number of pixels occupied by the house.

As it is was mentioned by Papathanassiou et al. (2013), the total landslide area is 3.17 km^2 meaning 31700 pixels and the area occupied by the house is 100 m^2 or 1 pixel. In addition, the probability of landslide occurrence conditioned on magnitude exceedance was estimated for the three most susceptible areas, coded as 10, 9 and 8, that cover 11.32% or 31.62 km^2 of the total area and 85% of the total slope instability one (Table 2). More quantitative data regarding the susceptibility classes can be found in Papathanassiou et al. (2013).

Table 2. Landslide susceptibility classes and relevant quantitative information

class	**km^2**	**pixels**	**% of the total area**	**% of the slope instability area**
10	1.65	16500	1.65	38.26
9	9.96	99600	3.02	32.44
8	20.01	200100	6.65	14.29

Taking into account the information listed in Table 2 and the published diagram of success and predicted rates curves of the susceptibility map (Papathanassiou et al., 2013), the Figure 3 and the relevant Table 3 are resulted. In particular, the plotted prediction curve was the outcome of the statistical analysis performed based on the inventory map of landslide in the island of Lefkada and is based on first and second column of the Table 3 in which the percentage of susceptible classes and the cumulative relevant percentage of landslide area are listed. Applying the equation 1 and taking into account the scenario that a house of 100m^2 is built within the delineated susceptible classes, the probabilities that this house will be part of the landsliding area can be estimated by the recommended by Chung and Fabri (2003) equation, and are listed in the third column of Table 3.

Having plotted this curve (Fig. 3), an exponential function can be developed to the empirical prediction rate curve based on the recommendations of Chung and Fabri (2003). The general equation of this fitted curve is:

$$y = 1 - e^{-a-bx} \tag{2}$$

Where x is the area representing the portion of the whole study area and a and b two parameters, which in our case were estimated as 0.07 and 14.91, respectively.

Thus, the fitted prediction-rate values were estimated based on this equation and are listed in the fourth column of Table 3. The relevant probabilities of the generation of a landslide within the covered areas (per class), calculated based on these values (4th column) and the equation 1, are listed in the fifth column of Table 3. In addition, a map of the spatial probability of earthquake-induced landslide is compiled and is shown in Figure 4.

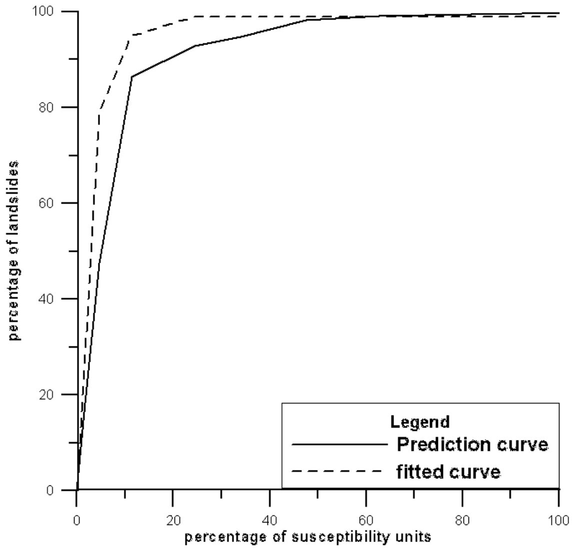

Figure 3.Continuous line shows the prediction curve and the dashed one the fitted curve.

Table 3. Conditional probability of slope failures within the delineated susceptibility classes

% cumulative	**cumulative portion (prediction curve value)**	**prob -empirical estimation (prediction curve)**	**fitted function**	**prob (fitted values)**
1.65	0.182	0.321	0.27095	0.455
4.67	0.292	0.104	0.13470	0.045
11.32	0.390	0.075	0.24842	0.044
24.36	0.065	0.005	0.21251	0.019
34.08	0.019	0.002	0.08546	0.009
47.58	0.034	0.003	0.09430	0.008
62.72	0.010	0.001	0.02702	0.002
81.86	0.003	0.000	0.04477	0.003
92.18	0.002	0.000	0.14737	0.014
99.89	0.000	0.000	0.09521	0.012

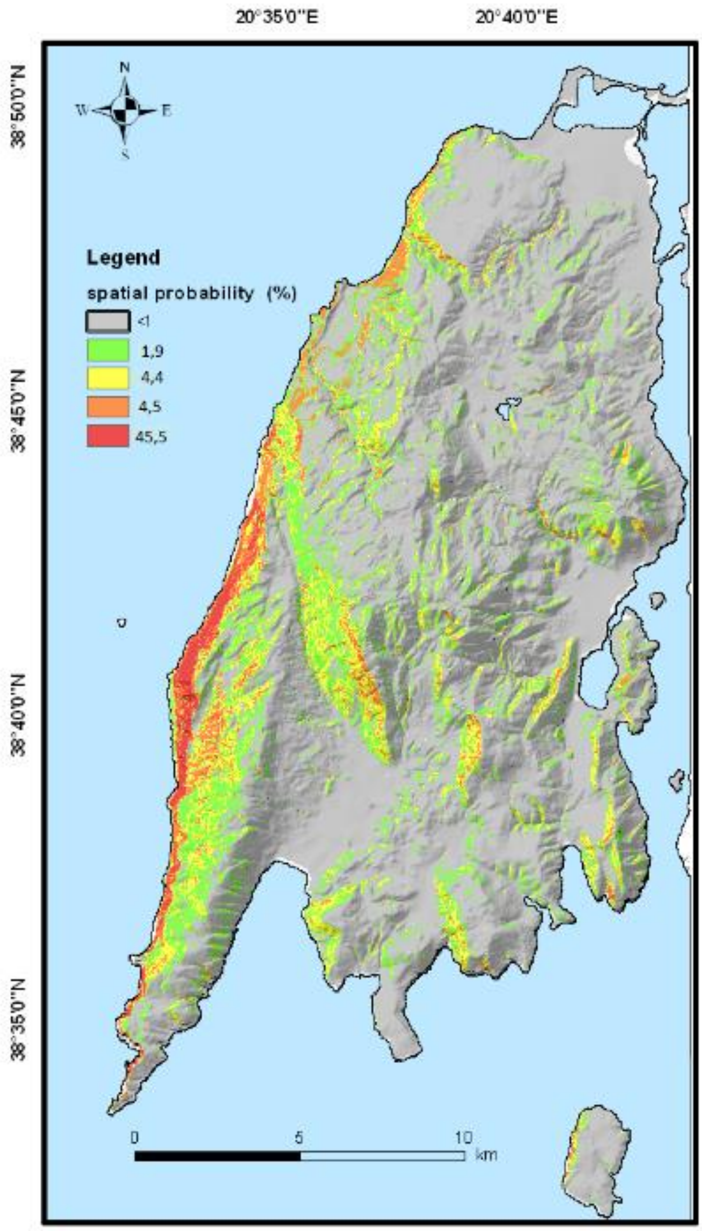

Figure 4. Spatial probability of earthquake-induced landslide based on the relevant susceptibility map

7. EVALUATING THE EARTHQUAKE-INDUCED LANDSLIDE ON THE ISLAND OF LEFKADA

In this section is presented the final step of the procedure towards the evaluation of landslide hazard. In particular, according to Jaiswal et al. (2010), a quantitative landslide hazard requires the estimation of three basic parameters; the magnitude probability, the temporal probability and the spatial probability. Using the above probabilities, the landslide hazard can be computed as the joint probability of landslide size, of landslide occurrence in an established time period and of the landslide spatial occurrence (Guzzetti et al., 2005; Jaiswal et al., 2010).

In the case of the island of Lefkada, the landslide hazard was estimated based on the two latter probabilities because the landslide size could not be accurately estimated. In particular, the landslide hazard was evaluated in terms of probabilities for return period between 10 to 500 years and the relevant values are listed in Table 4.

Table 4. Probability of earthquake-induced landslide hazard per earthquake scenario and period of years, within the most prone to slope failure areas in the island of Lefkada

	Earthquake scenario M=5.3 Probability hazard %				**Earthquake scenario M=6 Probability hazard %**			
	Susceptibility class							
period	10	9	8	7	10	9	8	7
10	9.46	0.93	0.92	0.39	17.06	1.68	1.65	0.7
20	10.74	1.06	1.04	0.44	29.44	2.91	2.86	1.21
50	10.83	1.07	1.05	0.44	35.99	3.55	3.49	1.48
75	10.83	1.07	1.05	0.44	37.49	3.70	3.64	1.55
100	10.83	1.07	1.05	0.44	37.81	3.73	3.67	1.56
500	10.83	1.07	1.05	0.44	37.9	3.74	3.68	1.57

The above probabilities should be used in conjunction with the landslide susceptibility map given the earthquake scenario per case. For example, land use planning for future development for a period of 50 years and an earthquake scenario of M6, should take into account that at the areas classified as susceptibility zone 10, a 36% probability of slope failure is expected. Moreover, taking into account the information provided by this study, the department of civil protection of the relevant ministry in Greece could prepare maps of open-access roads per earthquake scenario that would be used by the fire and the police department in case of an emergency.

8. CONCLUSIONS

The outcome of this study can be outlined in the following points:

- This study deals with the development of a quantitative model of earthquake-induced landslide hazard in the island of Lefkada. In particular, based on two thresholds of earthquake magnitude as they were defined for the area of Greece, the probabilities of landslide occurrence for a return period from 10 to 500 years were estimated for the whole island.
- Taken into account that this is the first time in Greece that the earthquake-induced landslide hazard is quantitatively estimated on a regional scale, this study could be used as an example for other areas in Greece or in seismically active countries around the world.
- Furthermore, the outcome of this study could be taken into account by the Greek government since it can be used as a base layer for risk analyses in the island of Lefkada and for emergency plans in case of an earthquake.

9. REFERENCES

Chung CJF, Fabbri A (2003). Validation of spatial prediction models for landslide hazard mapping. *Natural Hazard*, 30:451–472.

Cushing M (1985). Evolution structurale de la marge nord-ouest hellenique dans l'ile de Lefkada et ses environs (Greece nord-occidentale), *Ph. D. Thesis*, University de Paris-Sud (XI), Centre d' Orsay. France

Floris M, Bozzano F (2008). Evaluation of landslide reactivation: a modified rainfall threshold model based on historical records of rainfall and landslides. *Geomorphology*, 94: 40-57.

Ganas Ath, Elias P, Bozionelos G, Papathanassiou G, Avallone A, Papastergios A, Valkaniotis S, Parcharidis Is, Briole P (2016). Coseismic deformation, field observations and seismic fault of the 17 November 2015 M=6.5, Lefkada Island, Greece earthquake. *Tectonophysics*, 687:210-222.

Guzzetti F, Carrara A, Cardinali M, Reichenbach P (1999). Landslide hazard evaluation: a review of current techniques and their application in a multi-scale study, Central Italy. *Geomorphology*, 31:181-216.

Guzzetti F, Reichenbach P, Ardizzone F, Cardinali, M, Galli M (2005). Probabilistic landslide hazard assessment at the basin scale. *Geomorphology*, 72: 272–299.

Harp E, Keefer D, Sato H, Yagi H (2011). Landslide inventories: the essential part of seismic landslide hazard analyses. *Engineering Geology*, 22:9–21.

Jaiswal P, van Westen C (2009). Estimating temporal probability for landslide initiation along transportation routes based on rainfall thresholds. *Geomorphology*, 112:96-105.

Jaiswal P, van Westen C, Jetten V (2010). Quantitative landslide hazard assessment along a transportation corridor in southern India. *Engineering Geology*, 116: 236-250.

Louvari E, Kiratzi AA, Papazachos BC (1999). The CTF and its extension to western Lefkada Island. *Tectonophysics*, 308:223–236.

Papadopoulos GA, Plessa A (2000). Magnitude-distance relations for earthquake-induced landslides in Greece. *Engineering Geology*, 58:377- 386.

Papathanassiou G, Pavlides S, Ganas A (2005). The 2003 Lefkada earthquake: field observation and preliminary microzonation map based on liquefaction potential index for the town of Lefkada. *Engineering Geology*, 82:12–31.

Papathanassiou G, Valkaniotis S, Pavlides Sp (2011). Evaluation of the temporal probability of earthquake-induced landslides in the island of Lefkada, Greece. *Proceedings of the 2nd World Landslide forum, Rome, Italy*.

Papathanassiou G, Valkaniotis S, Ganas A, Pavlides Sp (2013). GIS-based statistical analysis of the spatial distribution of earthquake-induced landslides in the island of Lefkada, Ionian Islands, Greece. *Landslides*, 10(6): 771-783.

Papathanassiou G, Valkaniotis S, Ganas Ath, Grendas N, Kollia El (2017). The November 17th, 2015 Lefkada (Greece) strike-slip earthquake: Field mapping of generated failures and assessment of macroseismic intensity ESI-07. *Engineering Geology*, 220:13–30.

Pérouse E, Chamot-Rooke N, Rabaute A, Briole P, Jouanne F, Georgiev I, Dimitrov D (2012). Bridging onshore and offshore present-day kinematics of central and eastern Mediterranean: Implications for crustal dynamics and mantle flow. *Geochemical Geophysics Geosystem*, 13(9) doi:10.1029/2012GC004289.

Rondoyanni-Tsiambaou Th (1997). Les seismes et l'environnement géologique de l'île de Lefkade, Grèce : Passe et Future. In: Marinos et al. (eds) *Engineering Geology and the Environment*, Balkema, pp 1469-1474.

Rondoyanni Th, Sakellariou M, Baskoutas J, Christodoulou N (2012). Evaluation of active faulting and earthquake secondary effects in Lefkada Island, Ionian Sea, Greece: an overview. *Natural Hazards*, 61(2): 843-860.

Sachpazi M, Hirn A, Clement C, Haslinger F, Laigle Kissling E, Charvis P, Hello Y, Lepine JC, Sapin M, Ansorge J (2000). Western Hellenic subduction and Cephalonia transform: local earthquakes and plate transport and strain. *Tectonophysics*, 319:301–319.

Scordilis EM, Karakaisis GF, Karacostas BG, Panagiotopoulos DG, Comninakis PE, Papazachos BC (1985). Evidence from tranform faulting in the Ionian Sea: the Cephalonia island earthquake sequence of 1983. *Pure and Applied Geophysics*, 123(3): 387–397.

Varnes DJ (1984). Landslide hazard zonation: a review of principles and practice. UNESCO, France, pp 1–63.